

Power Losses in Magnetic Laminations with Hysteresis: Finite Element Modeling and Experimental Validation

Original

Power Losses in Magnetic Laminations with Hysteresis: Finite Element Modeling and Experimental Validation / Basso, V.; Bertotti, G.; Bottauscio, O.; Chiampi, Mario; Fiorillo, F.; Pasquale, M.; Repetto, Maurizio. - In: JOURNAL OF APPLIED PHYSICS. - ISSN 0021-8979. - 81:(1997), pp. 5606-5608.

Availability:

This version is available at: 11583/1398036 since:

Publisher:

AIP

Published

DOI:

Terms of use:

This article is made available under terms and conditions as specified in the corresponding bibliographic description in the repository

Publisher copyright

(Article begins on next page)

Power losses in magnetic laminations with hysteresis: Finite element modeling and experimental validation

V. Basso, G. Bertotti, O. Bottauscio, F. Fiorillo, and M. Pasquale
 IEN Galileo Ferraris, INFM and GNSM, C. so Massimo d'Azeglio 42, 1025 Torino, Italy

M. Chiampi and M. Repetto
 Politecnico di Torino, C. so Duca degli Abruzzi 24, 1029 Torino, Italy

Dynamic hysteresis loop shapes and magnetic power losses are studied in nonoriented Fe-Si laminations exhibiting significant excess losses. Measurements are carried out under controlled sinusoidal induction in the frequency range from 1 Hz to 1.6 kHz, at various peak inductions from 0.25 to 1.5 T. Excess losses are found to obey a $f^{3/2}$ law up to frequencies of 200–400 Hz, depending on peak induction. Beyond this limit, definite deviations are observed, due to eddy current shielding. Detailed information on the flux and field distribution in this high frequency regime is obtained by finite element solutions of Maxwell equations employing the dynamic Preisach model to describe quasi-static hysteresis and dynamic wall processes. The agreement between theoretical predictions and measurements is discussed. © 1997 American Institute of Physics. [S0021-8979(97)39708-4]

I. INTRODUCTION

A problem of increasing interest in applications is the accurate prediction of losses in magnetic cores operating in wide frequency intervals, under highly distorted flux waveforms. In such cases, the dynamic response of the core depends on the complex interplay of various factors (i) the hysteresis properties of the material; (ii) the incomplete flux penetration due to eddy current shielding and, (iii) the motion of domain walls, giving rise to excess losses.

In Ref. 1 we studied, both theoretically and experimentally, dynamic hysteresis and power losses in thick (1 mm) SiFe sheets, a case where excess losses play a negligible role and the interplay of static hysteresis and eddy current shielding could be analyzed in detail. Following these results, in this article we consider Fe-Si laminations whose thickness (0.33 mm) and grain size (of the order of 100 μm) are such that a significant excess loss contribution is expected. We have found that, up to frequencies of 200–400 Hz, excess losses follow the $f^{3/2}$ law predicted by the statistical loss theory.² Beyond this limit, a more complex behavior sets in, as a consequence of substantial eddy current shielding. In this high frequency regime, a numerical study was carried out, based, as recently proposed by several authors,^{3,4} on the dynamic Preisach model (DPM).⁵ DPM gives, in the form of a rate-dependent material constitutive law, a unified description of quasi-static hysteresis as well as dynamic domain effects responsible for excess losses. By inserting this constitutive law in a Maxwell equation finite element solver, it is possible to study in some detail the behavior of power losses and dynamic loop shapes when eddy current shielding and domain effects have comparable roles.

II. EXPERIMENTAL RESULTS

Measurements were performed on commercial (AST 27/35) nonoriented Fe-Si alloys (2.9 wt. % Si, 0.4 wt. % Al), with average grain size $s \approx 75 \mu\text{m}$. The lamination thickness was 0.334 mm. Epstein strips were cut at 0°, 30°, 60°, 90° angles to the rolling direction and inserted in the four frame legs in the order 0°, 30°, 90°, 60°, to emulate an isotropic

situation. Dynamic hysteresis loops, measured under controlled sinusoidal induction waveform at frequencies between 1 Hz and 1.6 kHz and peak inductions between 0.25 and 1.5 T, were recorded and the corresponding power losses were determined. A general overview of the measured energy loss per cycle versus frequency is given in Fig. 1, while details on the 1 and 1.5 T loss data are shown in Fig. 2.

The loss data were analyzed by means of the statistical loss theory,² which predicts for the power loss per unit mass in nonoriented steels

$$P = P_h + P_c + P_e = P_h + \frac{\pi^2}{6\delta} \sigma d^2 (B_p f)^2 + \frac{8}{\delta} \sqrt{\sigma G S V_0} (B_p f)^{3/2}, \quad (1)$$

where P_h is the quasi-static hysteresis loss, P_c is the classical loss, and P_e is the excess loss. As to the other symbols, $\delta = 7.65 \times 10^3 \text{ kg m}^{-3}$ is the mass density, $\sigma = 2.04 \times 10^6 \Omega^{-1} \text{ m}^{-1}$ is the electric conductivity, $G = 0.1357$, $S = 10^{-5} \text{ m}^2$ is the strip cross-sectional area, V_0 is a characteristic field describing the influence of the material microstructure on domain wall processes, f is the magnetization frequency, and B_p is the peak induction. The validity of this law can be tested by plotting $(P - P_c)/f$ as a function of $f^{1/2}$. This plot permits one to make a reliable estimate of the quantities P_h and V_0 , which, once inserted in Eq. (1), lead to the theoretical curves shown in Figs. 1 and 2. According to Ref. 2 when the correlation regions controlling the magnetization process coincide with individual grains, the field V_0 should be related to the grain size s and the static loss P_h through the relationship $V_0 \approx 2s^2 H_{\text{hyst}} \langle B_s \rangle / S B_p$, where $\langle B_s \rangle = 1.7 \text{ T}$ is the saturation flux density of an assembly of randomly oriented grains where rotation effects are negligible and H_{hyst} is an average coercivity value, $H_{\text{hyst}} = \delta P_h / 4 B_p f$. At 1.5 T, where $P_h = 38 \text{ mJ kg}^{-1}$, i.e., $H_{\text{hyst}} = 48.5 \text{ A m}^{-1}$, we find $V_0 \approx 0.06 \text{ A m}^{-1}$. This theoretical estimate is about one third of the experimental value of 0.17 A m^{-1} , which indicates that the actual size of the correlation regions is slightly larger than the grain size.

Figures 1 and 2 show that Eq. (1) is able to reproduce

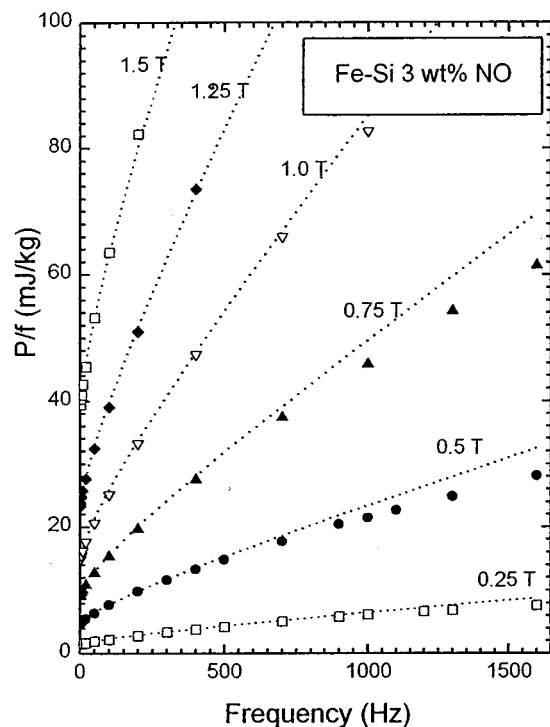


FIG. 1. Loss per cycle in nonoriented SiFe lamination. Symbols measured data. Dotted lines predictions of Eq. (1). Values of P_h (in mJ kg^{-1}) and V_0 (in A m^{-1}) used in calculations are as follows: 0.25 T: (1.45,0.07); 0.5 T: (4.45,0.1); 0.75 T: (8.6,0.12), 1 T: (14,0.14), 1.25 T: (22,0.15); 1.5 T: (38,0.17).

well the overall trend of measured losses. Yet, some significant discrepancies are observed. In general, the theoretical prediction overestimates the loss at low inductions and underestimates it at high inductions. The crossover is at 1 T,

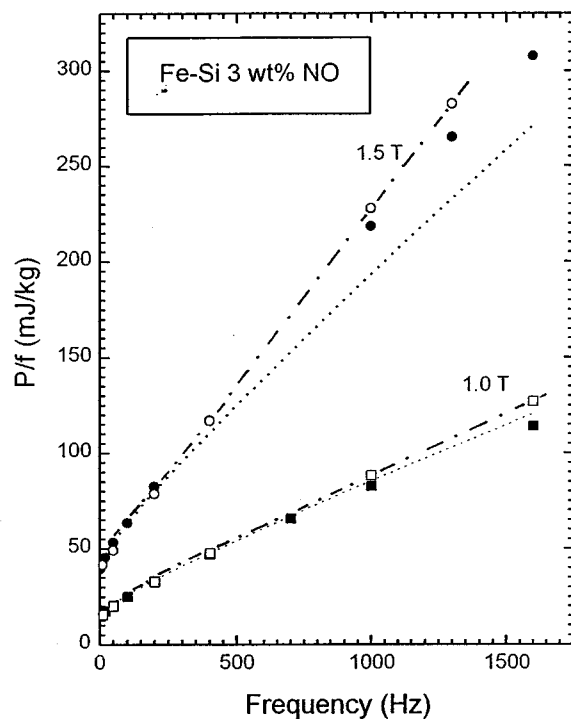


FIG. 2. Detail of loss per cycle at 1 and 1.5 T. Solid symbols and dotted lines: same as in Fig. 1. Open symbols: prediction of FEM calculation based on DPM.

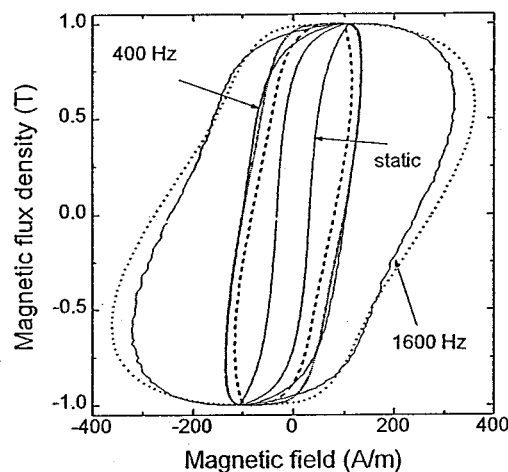


FIG. 3. Dynamic hysteresis loops at 1 T, for 0, 400, 1600 Hz. Continuous lines measurements. Dotted lines FEM prediction based on dynamic PM. Broken line. FEM prediction based on conventional PM.

where Eq. (1) is in remarkable agreement with experiments in the whole investigated frequency interval. At 1.5 T, the deviation of measured data from the $f^{1/2}$ law is quite significant when f exceeds ≈ 400 Hz. This is the consequence of distorted flux penetration due to eddy current shielding, a fact not taken into account by the theory leading to Eq. (1). In this regime, quasi-static hysteresis, classical eddy current shielding, and domain effects all have comparable roles and it is difficult to make accurate loss estimates without studying the full dynamic problem.

III. NUMERICAL STUDY

The dynamic flux and field distribution in the lamination cross-section is obtained by solving the equation

$$\nabla \times \nabla \times \tilde{\mathbf{H}}(x, t) = -\sigma \frac{\partial \tilde{\mathbf{B}}[\tilde{\mathbf{H}}(x, t)]}{\partial t} \quad (2)$$

for the electromagnetic \mathbf{H} field as a function of the depth x across a slab of thickness d and infinite width. The constitutive law $\mathbf{B}[\mathbf{H}]$ describes the hysteresis behavior of the mag-

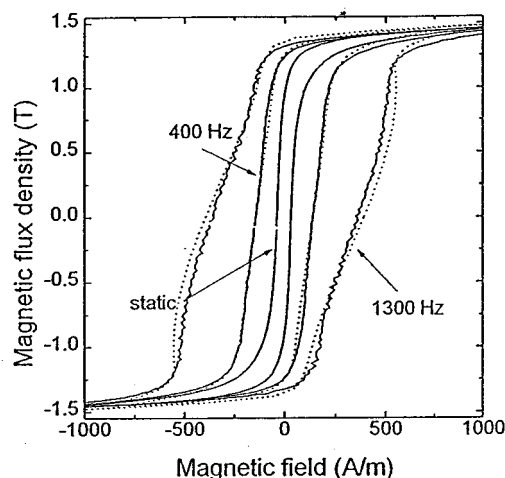


FIG. 4. Dynamic hysteresis loops at 1.5 T, for 0, 400, 1300 Hz. Continuous lines measurements. Dotted lines. FEM prediction based on dynamic PM.

netic material. It is assumed that \mathbf{B} and \mathbf{H} are always colinear and pointing along the longitudinal axis of the slab, which reduces $\mathbf{B}[\mathbf{H}]$ to a scalar relationship $B(H)$ between the field intensities. In this work, $B(H)$ is described by the DPM,⁵ which summarizes in a rate-dependent constitutive law quasi-static hysteresis and domain wall dynamic processes. Equation (2) is supplemented by the integral constraint $\int B[H(x,t)]dx = \Phi(t)$, where $\Phi(t)$ is proportional to the imposed sinusoidal magnetic flux.

The problem is linearized following the fixed point technique, which splits $B(H)$ into a linear term and a residual part $S[B(H) = \mu_T H + S]$, where S has to be iteratively estimated, starting from a trial value. Under periodic supply conditions, time dependencies are expanded in harmonic components, giving rise to a set of equations of the form

$$\nabla \times \nabla \times \mathbf{H}_k^{(n)} = -j\sigma\omega n \mu_T \mathbf{H}_k^{(n)} - j\sigma\omega n \mathbf{S}_{k-1}^{(n)} \quad (3)$$

with the constraint $\Phi^{(n)} = \int [\mu_T \mathbf{H}_k^{(n)} + \mathbf{S}_{k-1}^{(n)}] dx$. Here ω is the fundamental angular frequency, n is the harmonic order, k is the iteration index, and the field quantities are complex variables. At each iteration step, the finite element method (FEM), is employed to solve Eqs. (3), by dividing the slab thickness into 40 elements. This calculation gives the harmonic content of \mathbf{H}_k in each element. The time waveform $\mathbf{H}_k(t)$ is then determined by inverse fast Fourier transform (FFT). In order to compute the residual part $\mathbf{S}_k(t) = \mathbf{B}_k(t) - \mu_T \mathbf{H}_k(t)$, the flux density $\mathbf{B}_k(t)$ is evaluated through DPM. To this end, $\mathbf{H}_k(t)$ is applied as an input to DPM, starting from the demagnetized state, and, after the initial transients have died out (usually after 3–4 periods), the asymptotic periodic flux density output $\mathbf{B}_k(t)$ is obtained. Once $\mathbf{S}_k(t)$ is computed in each element, its harmonic content is calculated by FFT, the $\mathbf{S}_k^{(n)}$ terms in the right hand side of Eq. (3) are updated and the whole procedure is iterated until convergence is reached.

In the implementation of DPM, it is necessary to keep track of the time evolution of each point of the Preisach plane. The plane must be discretized in a number of elementary hysteresis operators sufficiently large to accurately reproduce the global behavior of the system, but on the other hand small enough to keep the computation time within reasonable limits. To this purpose, a new computationally fast algorithm was developed, where a single elementary hysteresis operator is associated with a finite region of the Preisach plane, and appropriate modified evolution equations for the whole region are introduced.⁶

The Preisach distribution $p(\alpha, \beta)$ was reconstructed from the recoil curve measured at 1.5 T.^{1,7,8} The DPM requires an hypothesis on the value of the parameter k , defined in Ref. 5 by the relation $\partial\varphi(\alpha, \beta; t)/\partial t = k(H - \alpha)$ [or $k(H - \beta)$], where $\varphi(\alpha, \beta; t)$ ($-1 \leq \varphi \leq 1$) describes the state of the point (α, β) of the Preisach plane and k measures the strength of the eddy current damping acting on moving domain walls. In Ref. 9 it is shown that, when the grain size controls the size of the correlation regions driving the magnetization process, k is expected to follow the relation $k \approx 1/\sigma G \langle B_s \rangle s^2$, which gives $k \approx 380 \text{ mA}^{-1} \text{ s}^{-1}$. In order to test this estimate, we carried out a set of simulations at 400 Hz and 1 T, even-

tually choosing for k the value at which the calculated and the measured loops had the same area. We found $k = 320 \text{ mA}^{-1} \text{ s}^{-1}$, which, when compared to the theoretical estimate $k \approx 380 \text{ mA}^{-1} \text{ s}^{-1}$, points again to correlation regions of size slightly larger than the grain size. The value $k = 320 \text{ mA}^{-1} \text{ s}^{-1}$ was kept constant in all subsequent simulations.

Calculations were performed at 10, 50, 200, 400, 1000, 1600 (1300 at 1.5 T) Hz, at 1 and 1.5 T peak inductions. In addition to the DPM approach used here, calculations based on the conventional PM method were also carried out, in order to quantify the importance of domain effects. Figures 3 and 4 show some of the measured hysteresis loops (continuous lines) together with the prediction of DPM calculations (dotted lines). The hysteresis loop calculated at 400 Hz, 1 T, by the conventional PM approach is also shown for comparison. The calculations based on the conventional PM gave unsatisfactory predictions for the loop shape in all the cases studied here. Domain effects should therefore be included in a correct procedure for the calculation of power losses by FEM in this type of laminations. The use of DPM definitely improves the agreement with measurements, even though, at high frequencies, the experimental loop shape appears more complicated than that which is predicted by the model. In any case, the loss prediction is basically correct, as illustrated by the results shown in Fig. 2 (open symbols), where, by the use of DPM, one can resolve discrepancies between the results provided by Eq. (1) (dotted lines) and measured losses (solid symbols).

As a final comment about the possible origin of some observed differences between simulations and measurements we might stress that the method used to determine the Preisach distribution was probably oversimplified. In particular, it does not take into account the field and induction dependence of the reversible permeability and the possible presence of mean-field effects.⁹ On the other hand, a more general problem resides in the fact that, with increasing frequency and increasing flux shielding by eddy currents, the magnetization process tends to become highly inhomogeneous in the lamination cross section. With such a rapid space variation of the flux distribution, it is not clear if one can still describe domain effects by a DPM-like local constitutive law, since the use of DPM necessarily implies some averaging of dynamic wall processes over regions containing many domains.

¹C. Appino, G. Bertotti, O. Bottauscio, M. Chiampi, F. Fiorillo, M. Repetto, and P. Tiberto, *J. Appl. Phys.* **79**, 4575 (1996).

²G. Bertotti, *IEEE Trans. Magn.* **24**, 621 (1988); F. Fiorillo and A. Novikov *ibid.* **26**, 2904 (1990).

³D. A. Philips, L. R. Dupre, and J. A. A. Melkebeek, *IEEE Trans. Magn.* **30**, 4377 (1994).

⁴L. L. Rouve, F. Ossart, T. Waeckerlé, and A. Kedous-Lebouc, *IEEE Trans. Magn.* **32**, 4219 (1996).

⁵G. Bertotti, *IEEE Trans. Magn.* **28**, 2599 (1992).

⁶O. Bottauscio, M. Chiampi, and M. Repetto, *Proc. 7th Int. IGTE Symposium, Graz, Austria, 1996*, p. 508.

⁷L. L. Rouve, T. Waeckerlé, and A. Kedous-Lebouc, *IEEE Trans. Magn.* **31**, 3557 (1995); V. Basso, M. Lo Bue, and G. Bertotti, *J. Appl. Phys.* **75**, 6577 (1994).

⁸G. Kadar, *J. Appl. Phys.* **61**, 4013 (1987).

⁹G. Bertotti and M. Pasquale, *IEEE Trans. Magn.* **28**, 2787 (1992).